Sustainable Energy & Fuels

Effects of Solids Retention Times on Electro-Selective Fermentation Using Scenedesmus acutus Biomass

Journal:	*Sustainable Energy & Fuels*
Manuscript ID	SE-ART-06-2020-000930.R1
Article Type:	Paper
Date Submitted by the Author:	19-Aug-2020
Complete List of Authors:	Liu, Yuanzhe; Arizona State University, Biodesign Swette Center of Environmental Biotechnology Lai, YenJung; Arizona State University, Biodesign Swette Center for Environmental Biotechnology Rittmann, Bruce; Arizona State University, Biodesign Swette Center for Environmental Biotechnology

Effects of Solids Retention Times on Electro-Selective Fermentation Using *Scenedesmus acutus* Biomass

Yuanzhe Liu[1], Yen-Jung Sean Lai[1], Bruce E. Rittmann[1]

Abstract

Electro-Selective Fermentation (ESF) is a means to enhance lipid wet extraction from microalgal biomass. The Solids Retention Time (*SRT*) is a decisive factor for maximizing lipid extraction and recovery, and effective ESF treatment requires a minimum *SRT* that needs to be determined. The hydraulic retention time (*HRT*) was manipulated to control the *SRT* in ESF treating *Scenedesmus acutus* biomass, since the *HRT* was almost equal to the *SRT* in our ESF experiments. An ESF process that started with a ~6-d *SRT* achieved high lipid extractability, but with relatively low lipid recovery. Shortening the *SRT* to ~2 d yielded slightly lower extractability, but nearly 100% lipid recovery and much higher volumetric productivity, compared to the 6-d *SRT*. Starting with an ~2-d SRT yielded much less extractable lipid production that did not increase after the SRT was extended to 6 d in a later stage. Microbial community analysis revealed lingering active fermenters when the *SRT* switched from long to short, but short to long *SRT* flushed out fermenters at first, although the fermenters were able to modestly recover after going back to the longer *SRT*. Thus, starting ESF with a longer *SRT* was important for selecting a microbial community able to achieve high lipid extractability, even though the subsequent shorter *HRT* achieved the highest production rate.

Keywords: Electro-Selective Fermentation (ESF); Microbial Electrolysis Cells (MEC); *Scenedesmus*; Lipids; Solid Retention Time (SRT); Principal Coordinates Analysis (PCoA)

1 Biodesign Swette Center of Environmental Biotechnology, Arizona State University, Tempe, AZ, 85287-5701 USA

1 Introduction

Microalga biofuel has been a great potential for alternative fuel. However, several technical barriers, such as high cost and lack of effective downstream processes, must be overcome (1–3). Electro-Selective Fermentation (ESF) is a novel technology that combines Selective Fermentation (SF) and a Microbial Electrolysis Cell (MEC) to enhance lipid wet extraction and promote desired fuel formula via "biohydrogenation" by β-oxidation from microalgae feeding biomass (FB) (4–6). *Scenedesmus* is one of the algae genera that are capable of accumulating intracellular lipids (7), but their cell wall, composed of trilaminar structure of glycosylated polypeptide, poses a strong barrier to the extraction of internal components, such as lipids and proteins (8,9). Hence, breaking down cell-wall carbohydrates and proteins can make the intracellular lipids more readily extractable. ESF has proven effective in degrading cellular protein of *Scenedesmus* biomass, thus exposing the lipids for wet extraction (4). In ESF, anode-respiring bacteria (ARB), which reside as a biofilm on an anode surface of a microbial electrolytic cell (MEC), scavenge the short-chain fatty acids (SCFA) generated in the fermentation process, and this lowers the SCFA concentrations. The electrons that ARB remove from the SCFAs flow from the anode to the cathode through the MEC's external circuit, ultimately reaching cathode where they reduce H_2O to generate H_2. Thus, ARB in ESF maximize electron utilization to energy-embodying products.

Liu et al. showed that ESF improved lipid wet extraction to about 25% (from < 1%), but this benefit came with a significant loss of total lipids (~30%) (4). The loss of lipids was associated with "biohydrogenation" through β-oxidation of unsaturated fatty acids, such as C18:1 and C18:3. β-oxidation cleaved off two carbon atoms from long-chain fatty acid (LCFA) molecules to form acetate and H_2 (10).

Acetate is the preferred substrate for ARB (11–13), and the generated acetate was converted to current at the anode, with H_2 harvested at the cathode. Thus, β-oxidation in ESF led to the benefits of additional saturated LCFA production, but also to the disbenefit of loss of total lipids. An improved ESF system would reduce total lipid loss and maintain the enhancements to lipid extraction and saturated-LCFA production.

A critical variable that determines performance of any microbiological system is the solids retention time (*SRT*), which is defined as the average time that biomass spends in the system (14). In ESF, the *SRT* of planktonic biomass can be manipulated by changing the hydraulic retention time (*HRT*) by changing the flow rate. As pointed out by Rittmann and McCarty, lipid fermenters have a slower growth rate compared to carbohydrate and protein fermenters (14). This means that a short *SRT*, associated with a short *HRT*, should selectively wash out planktonic lipid fermenters, while keeping protein and carbohydrate fermenters. Compared to SF, ESF was effective in enhancing lipid wet extraction and lipid "biohydrogenation" with *Scenedesmus acutus* biomass when the *HRT* was 5 days (4).

A potentially important factor is that the actual *SRT* in the ESF system may be larger than the *HRT* due to biofilm growth and accumulation. ESF involves a biofilm that is dominated by ARB, although other bacteria, such as protein and lipid fermenters, can inhabit the biofilm as well. For example, high-throughput sequencing by Liu et al. showed that *Geobacteraceae* (ARB), *Erysieplotrichaceae* (lipid fermenter), and *Porphyromonadaceae* (protein fermenter and lipid biohydrogenater) were present in the ESF biofilm in relatively high abundance (4). Thus, *SRT* values must be calculated on the basis of *HRT* and biofilm detachment in ESF. Establishing a proper *SRT*, achieved by implementing a specific *HRT*, may allow removal of carbohydrates

and protein, but conserve lipids. The ultimate outcome will be improved lipid wet-extraction, additional saturated fatty acid production, and better lipid conservation.

The specific goals of this research were to: 1) compare extractable-lipid production from *S. acutus* biomass for ESF with relatively long and short *SRTs*; 2) identify *SRT*s required for enhancing lipid extraction in *S. acutus* biomass, while minimizing lipid loss; and 3) link different lipid extractabilities with changes in the microbial community.

2 Material and Methods

2.1 MEC Reactors

Two flat-plate MEC reactors that followed the design of Ki et al. were used, but with removal of the cathodic serpentine structure (15). The MEC was constructed with multiple layers of transparent acrylic plates. The anode chamber had a volume of 200 mL, and the cathode chamber had a working volume of 66 mL. The anode was a carbon fiber (0.01-mm strand diameter, 2000 filaments, Goodfellows Cambridge Limited, Huntingdon, England) woven through a perforated titanium-plate mesh. The cathode was made of stainless-steel mesh (SS, type 316, mesh 80 * 80, 0.014cm of wire diameter, McMaster-Carr, Santa Fe Springs, CA, USA). The anode and cathode had geometric areas of 49 cm^2, but the actual area for biofilm attachment on the anode may have been greater than its geometric area due to the high specific area of the carbon fiber. An Ag/AgCl reference electrode (BASI Electrochemistry, West Lafayette, IN, USA) was installed at the center of the anode chamber from the top through a butyl-stopper with its tip ~3 cm above the bottom of the anode chamber and ~1cm from the surface of the carbon-fiber anode. An anion-exchange membrane (AEM) (AMI - 7001, Membranes International, New Jersey, USA) separated the anode and the cathode.

A biofilm dominated by ARB was accumulated on the anode surface of both MECs, prior to the experiments fed *S. acutus* biomass, by feeding a synthetic medium with a mixture of organic substrates (1970 mg/L sodium acetate, 380 mg/L sodium propionate, 200 mg/L sodium butyrate, 90 mg/L glucose, 140 mg/L Bovine Serum Albumin) and 1 mL/L of trace element solution (16) in a 80-mM phosphate buffer (pH = 7.5)). Initially, the feed synthetic medium (180 mL) was inoculated with anaerobic digester sludge (20 mL) from the Mesa Northwest Wastewater Reclamation Plant (MNWWRP, Mesa, AZ). Then, autoclaved synthetic medium was

continuously fed with an initial flow rate of 0.1 mL / min (*HRT* = 1.4 d), and the current was be monitored using the potentiostat connected to a computer with the EC-Lab software package. When the two reactors achieved a stable current density (~2 A/m^2), the flow rate was increased in increments of 0.1 mL/ min to increase the available flux of organic substrate to the biofilm, up to 0.5 mL/ min (*HRT* = 0.3d). Both reactors accumulated an active ARB biofilm with stable current density of ~5 A/m^2 after incubation of 12 days.

2.2. MEC Operation

The two MECs (denoted MEC-A and MEC-B) were operated with different *HRT* patterns. MEC-A had a 6-d *HRT* for 36 days and then a 2-d *HRT* for 12 days. MEC-B had a 2-d *HRT* for 12 days and then a 6-d *HRT* for 36 days. The ESF experiment was begun by filling the anode chamber with 180 mL of newly collected *S. acutus* biomass (80 mM PBS, pH = 7.0, 4.8 g VSS /L, Arizona State University, Tempe Campus, Tempe, AZ) inoculated with 20 mL WAS to ensure a diverse community of bacteria able for hydrolysis and fermentation. To achieve a 6-d *HRT*, 33 mL of anode effluent was removed at the end of each day, and 33 mL of fresh *S. acutus* feeding biomass (FB) was added immediately to re-establish the volume in the anode chamber. The 6-d *HRT* stage lasted for 36 days. From day 37 onwards, the *HRT* of MEC A was switched to 2 days, where 100 mL of effluent was replaced with FB each day until day 48. For MEC B, the reactor started with a 2-d *HRT*, where 100 mL of effluent were replaced daily from day 1 to 12. Then, the *HRT* was switched to 6 days, where the volume of effluent replacement was 33 mL per day until day 48. FB and effluent samples were collected every three days for the 2-d HRT stages and every six days at the 6-d *HRT* stages.

Volatile suspended solids (VSS), total chemical oxygen demand (TCOD), ammonia-nitrogen, protein, lipids, and short-chain fatty acids (SCFAs) in the FB and MEC effluents were assayed.

2.3 Analytical Methods

VSS was determined by methods described in sections 2540 B and E of *Standard Methods*(17). Total COD was measured using a HACH COD kit (HR+, concentration range 200-1,5000 mg/L). NH_4^+ was measured using HACH ammonium-N kit (concentration range 2 - 47 NH_4^+-N /L) (HACH Co., Loveland, CO, USA). After a sample was filtered through a 0.2-μm membrane (Pall Science, NY, USA), SCFAs were measured by high-performance liquid chromatography (HPLC) (LC-40, Shimadzu Corp, Columbia, MD, USA) equipped with an Aminex HPX-87H column (18).

Total and extractable lipids, characterized as fatty acid methyl esters (FAME) and expressed as COD values, were quantified for the solids using the method of Lai et al. (20). Total lipids were assayed by direct transesterification, which converted all algal triacylglycerides (TAGs) and diacylglycerides (DAGs) to fatty acid methyl esters (FAME). FAME concentrations were determined using a Shimadzu gas chromatography (GC-2010, Shimadzu Corp, Columbia, MD, USA) equipped with a Bio-Rad Animex HPX-87H column (Bio Rad Life Science, Hercules, CA, USA). Extractable lipids were measured by extraction with 100% hexane (H) followed by FAME analysis (5,19). Extractability (Ext%) was computed by dividing the extractable FAME by the total FAME of the corresponding FB (Eq. S1); saturation (Sat%) was computed by dividing the saturated FAME in the FB or effluent by the total FAME in the same sample (Eq. S2); and FAME recovery (Rec%) was computed by dividing the total FAME in an effluent sample by the total FAME of its corresponding FB (Eq. S3).

Total carbohydrates were determined by a modified phenol-sulfuric acid method developed by Laurens et al. (21). Total Protein was determined using a Bio-Rad protein kit (Bio-Rad, Hercules, CA, USA).

SCFAs, total protein, total carbohydrates, and total FAME concentrations obtained from these methods were converted mg COD /L to quantify the electron distribution in the solids.

2.4 Microbial Community Analysis

DNA samples from the FB, both reactor effluents, and both anode biofilms were extracted and analyzed for community analysis on day 36 (6-d *HRT* transition to 2-d *HRT*) and day 48 for MEC-A and on day 12 (2-d *HRT* transition to 6-d *HRT*) and day 48 for MEC-B. DNA was extracted using PowerSoil DNA isolation Kits (MoBio Laboratories, Inc, Carlsbad, CA, USA). Amplification and sequencing were performed by the Microbiome Analysis Laboratory, Arizona State University, using a MiSeq Illumina Sequencer, targeting the V4 Region of the 16S rRNA gene with primer set 515f/806r. 16S rRNA gene sequences were analyzed using the Quantitative Insights into Microbial Ecology software package (QIIME 2, version 2019.4, http://qiime2.org/). Principal coordinates analysis (PCoA) of the community structure in different samples was performed using EMPeror software package in the QIIME 2 system using weighted Unifrac method (22).

3. Results and Discussion

3.1 ESF Performance and *SRT*

The average current densities, obtained by dividing daily collected coulombs (1 d = 86400 s) and anode area (49 cm^2), are shown in Figures 1 (a) and (b). While both reactors, started up with fresh *S. acutus* FB, gave initial current densities of ~ 3 A/m^2, the current densities of the two reactors quickly diverged: For MEC-A (6-d *HRT*), the current density stabilized at ~1.2 A/m^2 at day 5, while the current density for MEC-B (2-d *HRT*) stabilized at ~ 2.0 A/m^2 at day 3. The average current densities had dramatic changes when the *HRT* was changed. For MEC-A, switching the *HRT* to 2d on day 37 led to an immediate increase in the current density to ~3 A/m^2; the current density slightly rose to ~3.3 A/m^2 on day 40 and then stayed stable for the rest of the experiment. For MEC-B, the *HRT* change to 6 d on day 12 caused a drop in the current density to ~1.3 A/m^2, although it gradually increased to ~2 A/m^2 by about day 37. The over-arching trend is that the 6-d *HRT* yielded lower current density than 2-d HRT, which indicates that a higher FB loading rate (caused by a shorter *HRT*) led to greater ARB activity brought about by a higher substrate flux to the ARB biofilm.

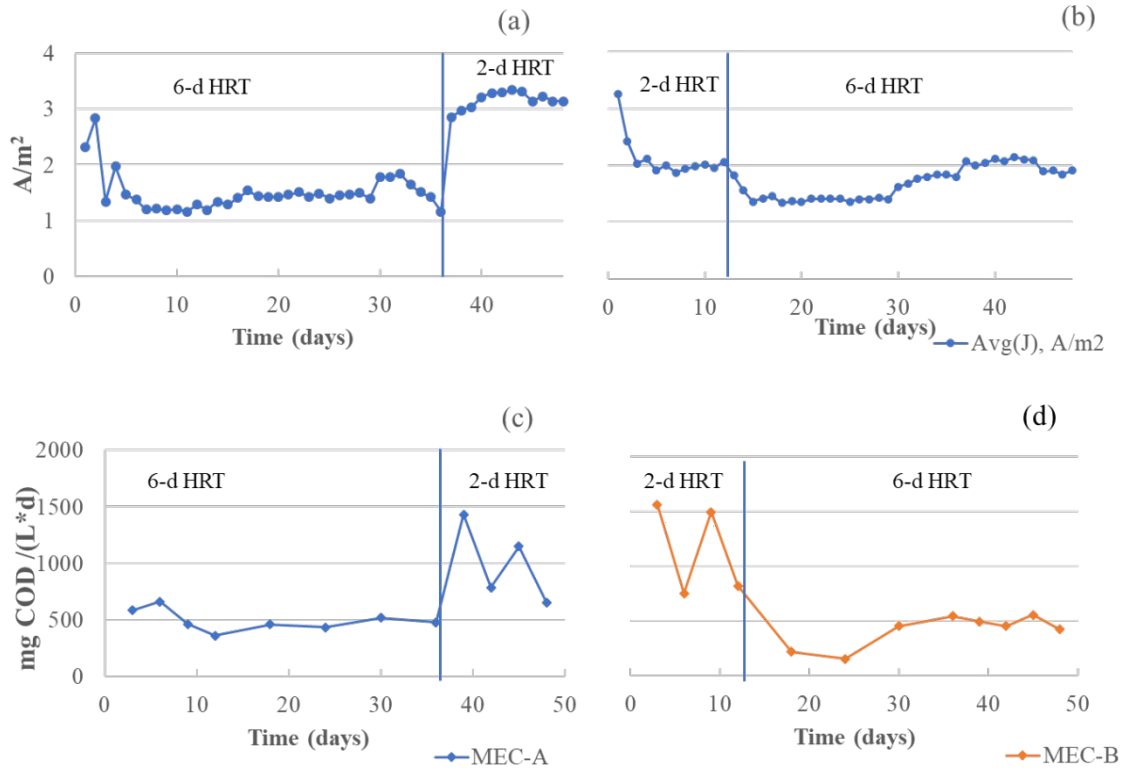

Figure 1. Trends of daily average current density for MEC-A (a) and MEC-B (b). Trends of daily COD removal rates for MEC A (c) and MEC- B (d). The *HRT*s and the times of *HRT* switches are shown.

The COD-removal rate was calculated by dividing the difference between FB-COD and effluent-COD (on the same day) by the *HRT*:

$$COD_{rate} = \frac{COD_{FB} - COD_{Eff}}{HRT} \qquad (Eq.\ 1)$$

where COD_{FB} (mg /L) is the FB-COD, COD_{Eff} (mg /L) is the effluent-COD on the same day, and *HRT* (d) is for the same day. Figures 1 (c) and (d) shows COD removal rates of MECs A and B. For MEC-A, the 6-d-*HRT* had an average COD removal rate of 500 ± 90 mg COD / L*d, but the *HRT* change to 2 d on day 36 increased the COD removal rate to 1010 ± 350 mg COD /L*d. Similarly for MEC-B, the average COD removal rate of 2-d *HRT* was 1160 ± 430 mg COD /L*d, but was 410 ± 150 mg COD /L*d for the 6-d *HRT*.

Calculations in part S1 of the Supplemental Information (SI) show that the overall *SRT*s of the ESF reactors were almost equal to the *HRT*s, since suspended biomass dominated biofilm biomass. Thus, *HRT* was an appropriate surrogate for the ESF's overall *SRT*.

3.2 FAME Extractability and Volumetric Productivity

FAME extractability for the biomass in the effluents of both MECs, along with the FB, are shown in Figure 2 (a) and (b). FB had low extractability for the whole period, ~ 5%. For MEC-A. The extractability rose rapidly after day 9, roughly linearly increased to ~25% at day 24, and then stayed stable to day 36, the end of the 6-d *SRT*. When the *SRT* of MEC-A was decreased to 2 d, the extractability decreased immediately to ~13% on day 39 and then stabilized at ~19%. For MEC-B, the extractability in the first 12 days, with the 2-d *SRT*, was similar to the FB, ~5%, which is different from the results obtained with 2-d *SRT* with MEC-A. After the *SRT* was switched to 6 d on day 13, the extractability began climbing, reaching ~11% on day 18 and eventually to ~22% by day 36. The lack of extractability enhancement with the initial *SRT* of 2 d suggests that the key hydrolytic and fermentative bacteria needed to degrade the protective layers of *S. acutus* could not accumulate, but were washed out with the 2-d *SRT*. When the longer *SRT* replaced the shorter HRT, these microorganisms were able to accumulate, which led to a breakdown of *S. acutus*'s protective structures. This explanation is consistent with the higher lipid extractability with the 6-d *SRT* for MEC-B than for MEC-A, because key hydrolytic and fermentative bacteria had been partially washed out during the 2-d stage of MEC A.

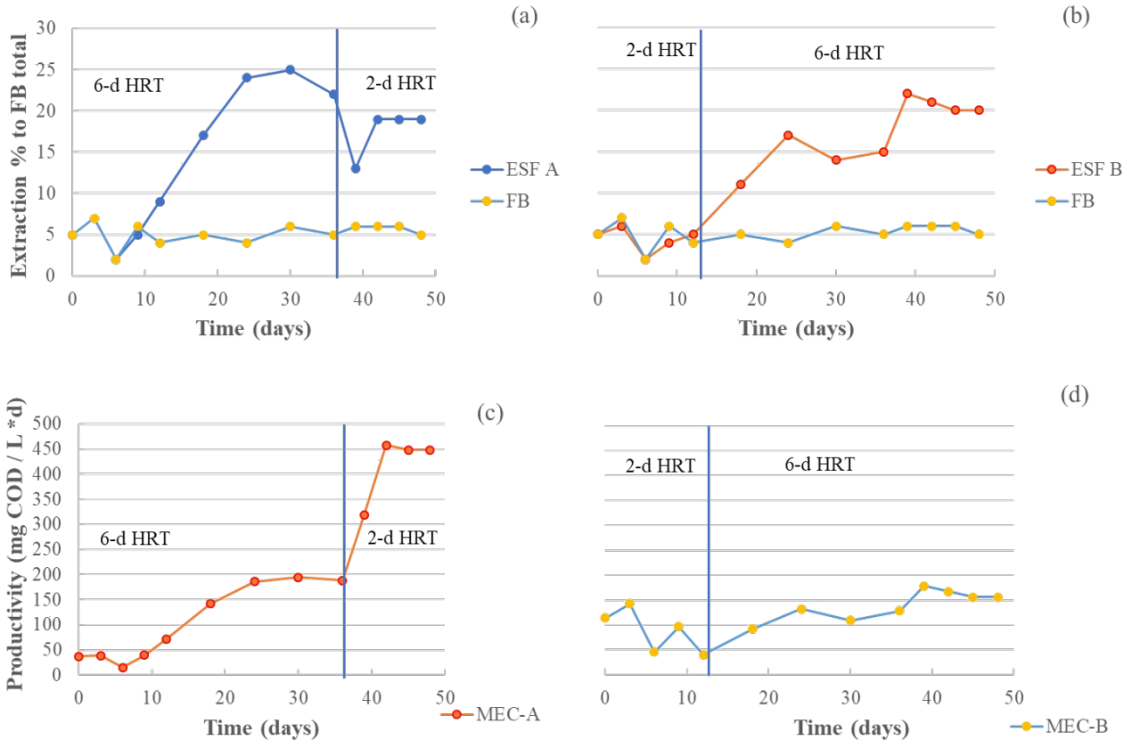

Figure 2. Trends of extractability for MEC-A (a) and MEC-B (b) and of FAME volumetric productivity for MEC-A (c) and MEC-B (d). The times of *HRT* switches are indicated. *SRT* is approximately equal to *HRT*.

For a specific day and reactor volume, the volumetric productivity of lipids ($Prod_{lipids}$, in mg COD / L•d), was calculated from:

$$Prod_{lipids} = COD_{FB} * Ext\% * Q_{eff} / V_r \qquad (Eq.\ 2)$$

where COD_{FB} is the total concentration of FAME in *S. acutus* FB (mg COD /L); Ext% is the extractability percentage for that day; Q_{eff} is the volume of effluent produced on the day (for a 6-d *SRT*, Q_{eff} = 33 mL / d; for a 2-d *SRT*, Q_{eff} = 100mL / d); and V_r is the volume of the reactor (200 mL). Figures 2 (c) and (d) shows that the trends of FAME recovery differed from the trends for extractability. For MEC-A, the FAME productivity was stable between days 0-12 at ~50 mg COD /L*d and then increased to ~240 mg COD /L*d on day 24. Switching the *HRT* to 2 d caused an immediate increase in productivity, reaching ~450 mg COD/L*d on day 39, the top productivity achieved by MEC-A. For MEC-B, the FAME productivity was 120 mg COD /L*d at the start, declining to ~40 mg COD /L*d on day 12 before the *SRT* was switched to 6d. Then, the productivity increased and reached peak at 180 mg COD /L*d between day 39 and day 48. The lipid productivity in MEC-B never reached the values of MEC-A with a 6-d *SRT*. This reinforces that having the 6-d *SRT* after the 2-d *SRT* in MEC-B did not restore a microbial community as effective at hydrolytic and fermentative functions. In general, a lower *SRT* after a longer *SRT* supported higher volumetric productivity, but modestly lower lipid extractability; however, starting the MEC with a short *SRT* flushed out fermenters, which were not restored once the *SRT* was extended to 6 d. Thus, as long as the MEC had been started with a long *SRT*, which selected a suitable microbial community that was able to ferment protective layer and expose lipids, switching to a shorter *SRT* retained the fermenters so that high extractability could continue. Thus, volumetric lipid productivity was higher, since the extractability did not dramatically shrink.

SRT also had an influence on FAME recovery for the two MECs, as shown in Figure 3. The FAME recovery percentage started low for MEC-A, with a 6-d *SRT*, possibly caused by algae biomass attachment to the anode biofilm, as seen in Liu et al. (5). Then, it increased to and peaked at ~95% on day 30. At this point, MEC-A had the highest FAME extractability (Fig. 2(a)) and low FAME loss, perhaps because the newly exposed algal-lipid has not accumulated a substantial amount of lipid fermenters. After the *SRT* switch to 2 d, the FAME recovery again approached 100% on day 48, when extractability was high at ~20%. Perhaps the lipid fermenters (but not protein and carbohydrate fermenters) were washed out by the *SRT* of 2 d, fulfilling the potential to achieve high extractability and high lipid recovery, with a short-enough *SRT* (2 d).

MEC-B displayed high, but unstable FAME recovery with the 2-d *SRT* (~65 to ~100%). The lower values may have been due to a combined effect of biomass attachment to the anode and low lipid degradation with a short *SRT*. After the *SRT* switch to 6 d, FAME recovery initially rose to >100% (day 24), and this may have been caused by removal of lipids that had attached to the anode. FAME recovery then decreased and stabilized at ~80% on day 30. Similar to MEC-A, the trends for MEC-B suggest that lipid degraders and fermenters were washed out with the 2-d *SRT*. However, the fermenters were able to regrow after the *SRT* was switched to 6 d.

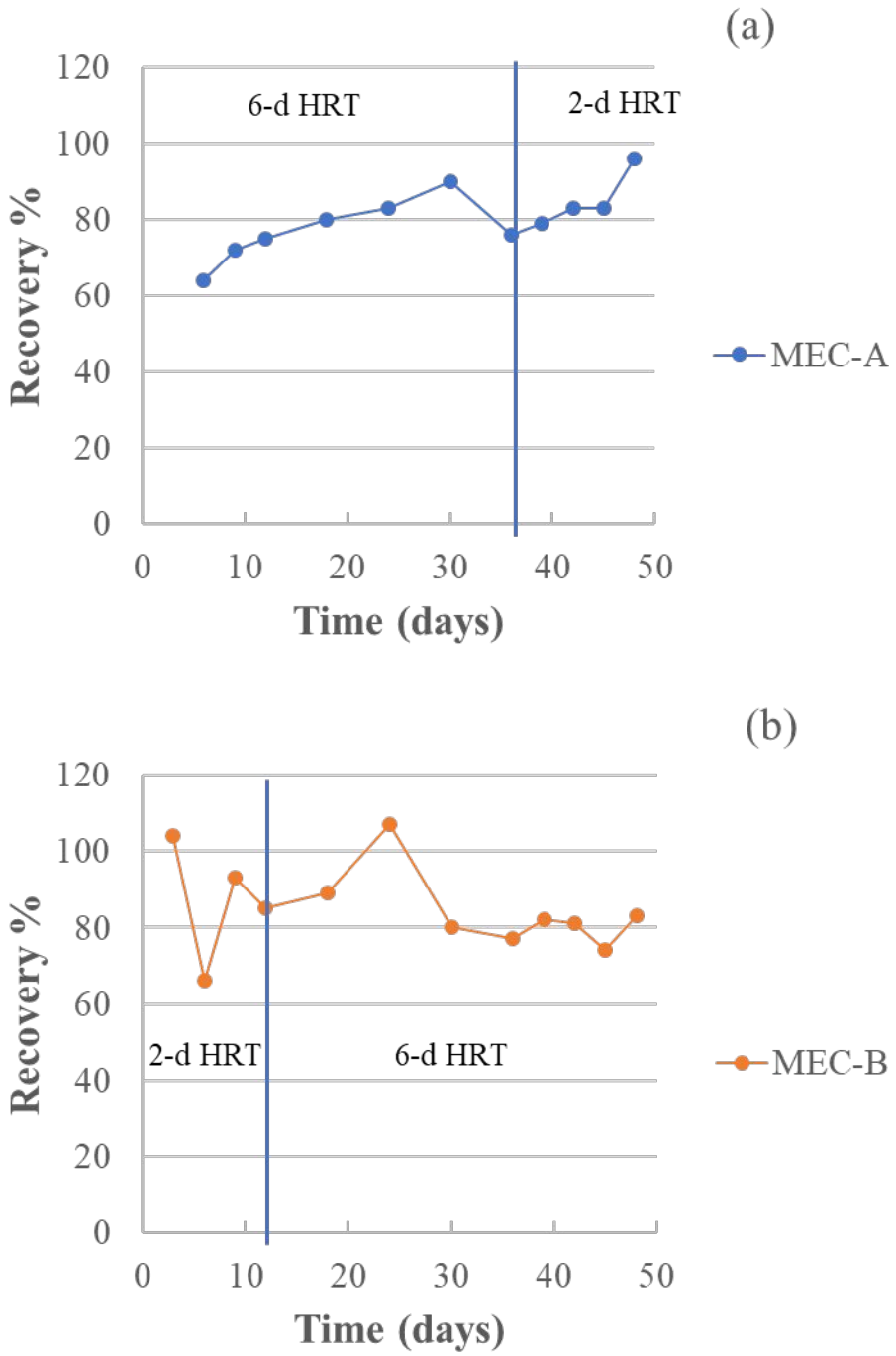

Figure 3. Trends of FAME recovery percentage for MEC-A (a) and MEC-B (b). The times of *HRT* switches, with *HRT*s applied are shown. The *SRT* is approximately equal to the *HRT*.

3.3 Short-Chain Fatty Acids (SCFAs)

Concentrations of SCFAs in the effluents of MEC-A and MEC-B, expressed in mg COD /L, are shown in Figure 4. Significant SCFA species were formate, acetate, propionate, butyrate, valerate, and caproate. Since caproate exhibited unique trends, Figures 4 (b) and (d) shows caproate and total SCFAs excluding caproate.

In MEC-A, total SCFA was high at the start, 1600 mg COD /L, and >90% was caproate. Total SCFA decreased rapidly, mostly caused by the decrease of caproate, reaching nearly zero after 36 days of operation at the 6-d *SRT* reaction; the almost-complete removal of SCFAs demonstrates strong ARB activity. After the *SRT* was switched to 2 d, total SCFA modestly increased, to ~400 mg COD /L on day 48, and caproate contributed ~ 50%. The total SCFA concentration rebounded, and current density was higher after the *SRT* switch (Figure 1. (a)). Both factors demonstrate that the 2-d *SRT* allowed a higher volumetric fermentation rate (Figure 1 (c)) that produced more SCFAs and, consequently, higher current.

For MEC-B, total SCFA started lower (~800 mg COD /L) than MEC-A, and the majority (~75%) was caproate. The initial 2-d *SRT* in MEC-B showed a modest declining trend of total SCFA and caproate out to day 12, and this may indicate a gradual accumulation of more ARB. After the *SRT* was increased to 6 d, the declining trend of total SCFA accelerated, again mostly caused by rapidly declining caproate. Total SCFA reached ~200 mg COD /L on day 48, and the majority was still caproate (up to 90%).

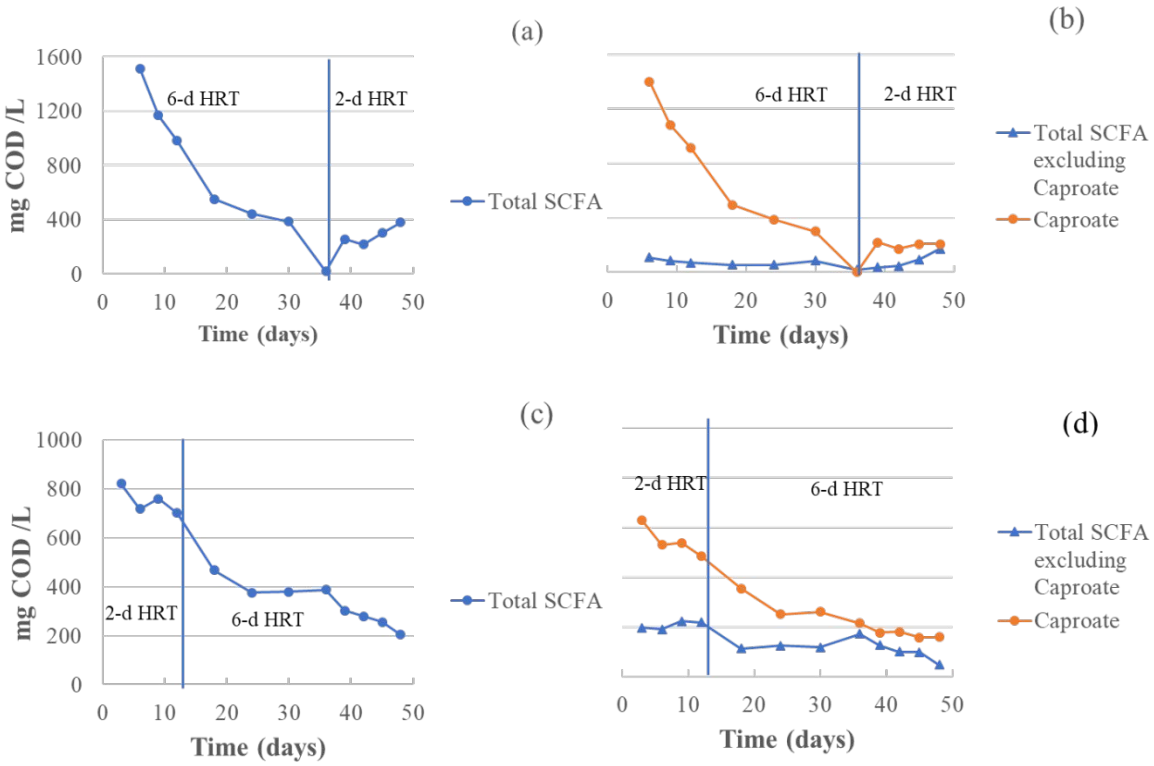

Figure 4. Trends of SCFA concentrations, in mg COD/L: total SCFA in MEC-A (a), Caproate and SCFA excluding caproate in MEC-A (b), total SCFA in MEC-B (c), caproate and SCFA excluding caproate in MEC-B (d). The points of *HRT* switch, as well as the implemented *HRT*, are shown. *SRT* is approximately equal to the *HRT*.

3.4 Microbial Community Structure

Microbial community structures at the family level for the FB, the MEC effluents, and MEC biofilms were determined using high-throughput sequencing. To determine if the different sources had distinct community structures, Principal Coordinates Analysis (PCoA) was performed. The results, shown in Figure 5, clearly show three clusters: FB to the far right on the PC1 axis (56.8%), the biofilms on the far left on the PC1 axis, and the MEC effluents in the middle of the PC1 axis, but higher on the PC2 axis (19.1%). Thus, the communities in FB, MEC effluent suspended biomass, and MEC biofilms were distinct.

Some trends appear within the three groups. FB had a systematic movement down on the PC2 axis due to its storage, but almost no movement along the PC1 axis. Because the PC2 axis presented a small portion of the total variance (19.1%), the movement was not a sign of a major change in community structure.

In the cluster of the effluent suspended biomass, MEC-A shifted significantly on both axes between d12 and d36 with 6-d *HRT*, but the subsequent shift between d36 and d48 (to a 2-d *HRT*) was smaller along the PC1 axis and almost negligible along the PC2 axis. This indicates that 6-d *HRT* caused a bigger shift in the microbial community than did the 2-d *SRT*. The MEC-B community clearly moved left along the PC1 axis between d12 and d36, but the subsequent move between d36 and d48 (6-d *SRT*) was negligible. The shifts for MEC-B (started with the 2-d *SRT*) were smaller than for MEC-A (started with the 6-d *SRT*), especially between d36 and d48. Thus, the change in the microbial community was smaller when the *HRT* was increased. This indicates that the recovery of slow-growing bacteria in MEC-B was poor when the 6-d *SRT* was implemented after start up with the 2-d *SRT*.

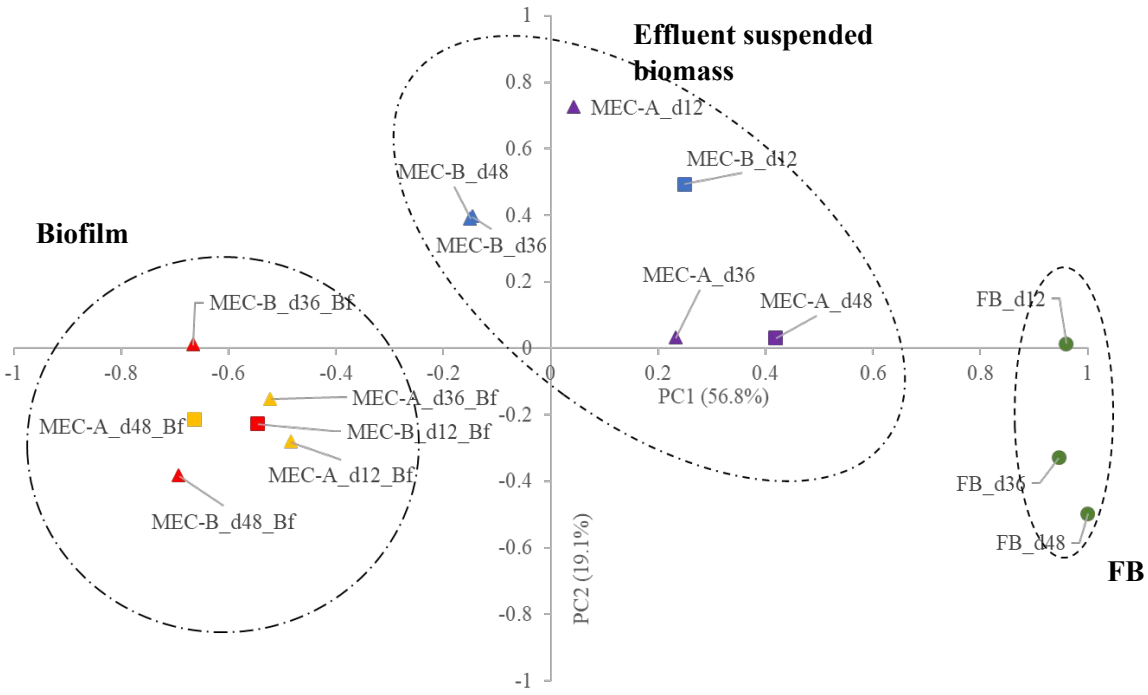

Figure 5. Principal Coordinates Analyses (PCoA) for microbial communities of FB, MEC effluents, and biofilms. Symbol shapes denote the *SRT* at the time the sample was taken: 6 d (▲) or 2 d (■). Color denotes the sample type: purple for MEC-A effluent, blue for MEC-B effluent, orange for MEC-A biofilm, and red for MEC-B biofilm. A green circle denotes FB. The designation dxx indicates the day on which the sample was taken. The percentages in the axis labels represents the percentages of variations explained by the two principal coordinates; axes values denote degree of variance within the range of -1 and 1.

Microbial community structures at the family level in the MEC-A effluents, MEC-A biofilm, and the FB are presented in Figure 6, which also identifies known functions of each family. Parallel presentations for MEC-B are in the Supplemental Information.

The FB (Fig. 6(a)) had a high abundance of *Chlamydomonadaceae*, which corresponds to the chloroplast DNA of *S. acutus*; however, endogenous degradation occurred during FB storage, and the DNA of *Chlamydomonadaceae* decreased between days 12 and 48. The abundance of *Pseudomonadace* greatly increased with time. *Pseudomonadaceae* potentially includes cryophilic bacteria capable of degrading *S. acutus* cellular structure (23).

In both MECs (Fig. 6(b) and Fig. S1(a)), *Chlamydomonadaceae* was substantially less with the 6-d *SRT*, compared to the 2-d *SRT*. Lower *Chlamydomonadaceae* abundance also was associated with the higher lipid extractability with the longer *SRT* (Fig. 1). Both trends are consistent with greater breakdown of the cell wall of *Chlamydomonadaceae* with the longer *SRT*.

One known lipid hydrogenator, *Erysipelotrichaceae* (4), was in the FB. It, along with the other known lipid fermenter, *Porphyromonadaceae*, greatly increased in both MECs on day 12, although they declined after day 12. The decline may have been due to these two lipid hydrogenators being slow growers that were washed out regardless of *SRT* being 6 d or 2 d. Hence, these lipid fermenters' population could be controlled via an adequate *SRT*. *Porphyromonadaceae* had less decline than *Erysipelotrichaceae*, probably due to the fact that it can also metabolize sugars when usable lipids are not available as substrates (24).

All the known fermenters present in the FB, except *Cytophaceae*, accumulated in the MECs, especially *Pseudomonadaceae*, which had a dramatic increase up to as high as 28% in MEC-A. These FB-indigenous fermenters accumulated in the MECs regardless of long or short *SRT*, since

they had a fast-enough growth rate to withstand washout. In contrast, *Synergistaceae* and all *Bacteroidiales*, including *Porphyromonadaceae*, which are non-indigenous fermenters, were important for an *SRT* of 6 d, but slightly declined for the 2-d *SRT*. This indicates that these fermenters were promoted by the long *SRT* (6-d). The shorter *SRT* (2-d), though not promoting their growth, did not have a strong flush-out effect for them. In summary, the fermenters' growth was strongly supported by the 6-d *SRT*, but they could withstand completely washout with the 2-d *SRT*. The high lipid extractability in MEC-A with 6-d and 2-d S*RTs* may have been associated with the continued persistence of these fermenters.

The anodes of both MECs displayed typical ARB biofilms, with by far the largest number of sequences belonged to *Geobacteraceae*, a widely recognized ARB (11,25,26). The abundance of *Geobacteraceae* was at least 31%, similar to the value in Liu et al. (4), indicating a healthy and electrochemically active biofilm. The biofilms also harbored small fractions of all of the microbial types detected in the suspension, while the effluents of both MECs had small numbers of *Geobacteraceae* that were not in the FB. Hence, the biofilm and suspended communities exchanged microorganisms. The biofilms also hosted increasing abundance of *Erysipelotrichaceae* and *Porphyromonadaceae*, showing that these lipid fermenters were thriving in the biofilm. Abundance of bioavailable lipid substrates attached to the anode might be the cause to this phenomenon, which is similar to the observation presented in Liu et al. (4).

The only methanogen detected was *Methanocorpusculaceae*, a H_2-oxidizing family, and it always comprised less than 10% of abundance. No acetate-consuming methanogens were present, as they were out-competed by the ARB (18), leaving H_2-consuming methanogens as the only methanogens.

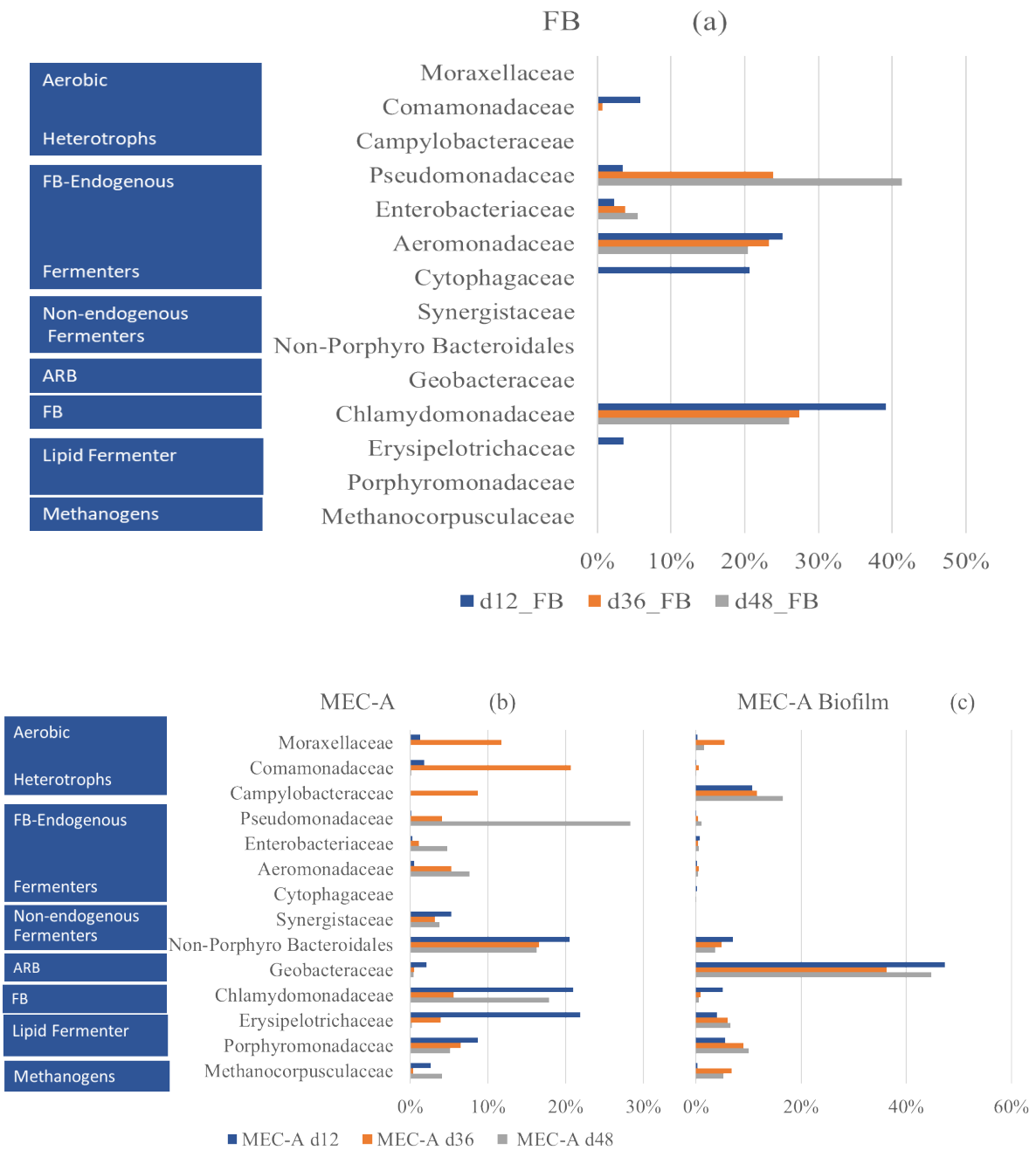

Figure 6. Phylogenetic profiling of the suspended biomass in the FB (a), MEC-A effluent suspension (b), and MEC-A biofilm (c) at the family level. Parallel phylogenic profiles of MEC-B effluent and biofilm are shown in Figure S1 in the Supplemental Information. The horizontal axis presents the percentage abundance of the families based on the total reads of the 16S rRNA gene. Functions associated with each family are shown to the left.

4. Conclusion

ESF enhanced lipid extraction from *S. acutus* biomass, and different MEC *HRT*s, which were almost equal to the overall *SRT*s, led to different results for lipid extraction and other performance parameters. Starting the MEC with a 6-d *SRT* attained the highest lipid extractability (25%); shifting that MEC to a 2-d *SRT* gave the highest lipid productivity per unit reactor volume (450 mg /L * d). Starting the MEC with a 2-d *SRT* impaired the enhancement of lipid extractability, which was not recovered when the 6-day *SRT* was implemented.

Principal Coordinates Analysis revealed that the communities of the FB, MEC effluent, and MEC biofilms were distinct, with the microbial community in the MEC effluent most strongly affected by the change in *SRT*. The 6-d *SRT* had more lipid fermenters (*Erysipelotrichaceae* and *Porphyromonodaceae*), but both *SRT*s flushed out these slow-growing lipid fermenters. Protein fermenters, such as *Syneristaceae*, *Pseudomonadaceae*, and *Enterobacteriaceae*, were flushed out with the 2-day *SRT* and could not recover after the switch to a longer *SRT*. The microbial community of the biofilms, which was not affected systematically by the *SRT*, was dominated by well-known ARB, but also contained the same fermenters as in the suspended biomass.

Taking into account all the results, ESF operation was able to enhance lipid extractability and productivity when the MEC's had an initial *SRT* of 6 d that was switched to 2 d. The 6-d *SRT* established a community containing protein fermenters, and the 2-d *SRT* washed out the lipid fermenters.

References

1. Rittmann BE. Opportunities for renewable bioenergy using microorganisms. Biotechnol Bioeng. 2008;100(2):203–12.
2. Pierobon SC, Cheng X, Graham PJ, Nguyen B, Karakolis EG, Sinton D. Emerging microalgae technology: A review. Sustain Energy Fuels. 2018;2(1):13–38.
3. Sills DL, Paramita V, Franke MJ, Johnson MC, Akabas TM, Greene CH, et al. Quantitative uncertainty analysis of life cycle assessment for algal biofuel production. Environ Sci Technol. 2013;47(2):687–94.
4. Liu Y, Lai Y-JS, Barbosa TS, Chandra R, Parameswaran P, Rittmann BE. Electro-selective fermentation enhances lipid extraction and biohydrogenation of Scenedesmus acutus biomass. Algal Res [Internet]. 2019;38:101397. Available from: http://www.sciencedirect.com/science/article/pii/S2211926418306362
5. Liu Y, Sean Lai Y-J, Rittmann BE. Increased anode respiration enhances utilization of short-chain fatty acid and lipid wet-extraction from Scenedesmus acutus biomass in Electro-Selective Fermentation. Renew Energy [Internet]. 2019 Oct 12 [cited 2019 Oct 20]; Available from: https://www.sciencedirect.com/science/article/abs/pii/S0960148119315356
6. Knothe G. Analyzing biodiesel: standards and other methods. J Am Oil Chem Soc [Internet]. 2006;83(10):823–33. Available from: https://doi.org/10.1007/s11746-006-5033-y
7. Sivaramakrishnan R, Suresh S, Pugazhendhi A, Mercy Nisha Pauline J, Incharoensakdi A. Response of Scenedesmus sp. to microwave treatment: Enhancement of lipid, exopolysaccharide and biomass production. Bioresour Technol [Internet]. 2020;312(May):123562. Available from: https://doi.org/10.1016/j.biortech.2020.123562
8. Allard B, Templier J. High molecular weight lipids from the trilaminar outer wall (TLS)-containing microalgae Chlorella emersonii, Scenedesmus communis and Tetraedron minimum. Phytochemistry. 2001;57(3):459–67.
9. Voigt J, Stolarczyk A, Zych M, Malec P, Burczyk J. The cell-wall glycoproteins of the green alga Scenedesmus obliquus. The predominant cell-wall polypeptide of Scenedesmus

obliquus is related to the cell-wall glycoprotein gp3 of Chlamydomonas reinhardtii. Plant Sci [Internet]. 2014;215–216:39–47. Available from: http://dx.doi.org/10.1016/j.plantsci.2013.10.011

10. Cavaleiro AJ, Pereira MA, Guedes AP, Stams AJM, Alves MM, Sousa DZ. Conversion of Cn-Unsaturated into Cn-2-Saturated LCFA Can Occur Uncoupled from Methanogenesis in Anaerobic Bioreactors. Environ Sci Technol. 2016;50(6):3082–90.

11. Miceli JF, Garcia-peña I, Parameswaran P, Torres CI, Krajmalnik-brown R. Combining microbial cultures for efficient production of electricity from butyrate in a microbial electrochemical cell. Bioresour Technol [Internet]. 2014;169:169–74. Available from: http://dx.doi.org/10.1016/j.biortech.2014.06.090

12. Mahmoud M, Parameswaran P, Torres CI, Rittmann BE. Fermentation pre-treatment of landfill leachate for enhanced electron recovery in a microbial electrolysis cell. Bioresour Technol [Internet]. 2014;151:151–8. Available from: http://dx.doi.org/10.1016/j.biortech.2013.10.053

13. Ki D, Parameswaran P, Popat SC, Rittmann BE, Torres CI. Effects of pre-fermentation and pulsed-electric-field treatment of primary sludge in microbial electrochemical cells. Bioresour Technol [Internet]. 2015;195:83–8. Available from: http://dx.doi.org/10.1016/j.biortech.2015.06.128

14. Rittmann BE, McCarty PL. Environmental Biotechnology: Principles and Applications [Internet]. Tata McGraw Hill Education Private Limited; 2001. (McGraw-Hill series in water resources and environmental engineering). Available from: https://books.google.com/books?id=qM43AwAAQBAJ

15. Ki D, Popat SC, Torres CI. Reduced overpotentials in microbial electrolysis cells through improved design, operation, and electrochemical characterization. Chem Eng J. 2016;287:181–8.

16. Lee H-S, Parameswaran P, Kato-Marcus A, Torres CI, Rittmann BE. Evaluation of energy-conversion efficiencies in microbial fuel cells (MFCs) utilizing fermentable and non-fermentable substrates. Water Res. 2008 Mar;42(6–7):1501–10.

17. APHA. Standard Methods for the Examination of Water & Wastewater, 20th edition.

Washington DC: American Public Health Association; 2016.

18. Parameswaran P, Torres CI, Lee H-S, Krajmalnik-Brown R, Rittmann BE. Syntrophic interactions among anode respiring bacteria (ARB) and Non-ARB in a biofilm anode: electron balances. Biotechnol Bioeng [Internet]. 2009;103(3):513–23. Available from: http://www.ncbi.nlm.nih.gov/pubmed/19191353

19. Lai YJS, McCaw A, Ontiveros-Valencia A, Shi Y, Parameswaran P, Rittmann BE. Multiple synergistic benefits of selective fermentation of Scenedesmus biomass for fuel recovery via wet-biomass extraction. Algal Res [Internet]. 2016;17(May):253–60. Available from: http://dx.doi.org/10.1016/j.algal.2016.05.001

20. Lai YS, Parameswaran P, Li A, Aguinaga A, Rittmann BE. Selective fermentation of carbohydrate and protein fractions of Scenedesmus , and biohydrogenation of its lipid fraction for enhanced recovery of saturated fatty acids. Biotechnol Bioeng. 2016;113(February 2016):320–9.

21. Laurens LML, Dempster TA, Jones HDT, Wolfrum EJ, Wychen S Van, Mcallister JSP, et al. Algal Biomass Constituent Analysis: Method Uncertainties and Investigation of the Underlying Measuring Chemistries. Anal Chem. 2012;84(4):1879–87.

22. Vázquez-Baeza Y, Pirrung M, Gonzalez A, Knight R. EMPeror: A tool for visualizing high-throughput microbial community data. Gigascience. 2013;2(1):2–5.

23. Reddy GSN, Matsumoto GI, Schumann P, Stackerbrandt E, Shivaji S. Psychrophilic pseudomonads from Antarctica: Pseudomonas antartica sp. nov., Pseudomonas meridiana sp. nov. and Pseudomonas proteolytica sp. nov. Int J Syst Evol Microbiol. 2004;54(3):713–9.

24. Hahnke S, Maus I, Wibberg D, Tomazetto G, Pühler A, Klocke M, et al. Complete genome sequence of the novel Porphyromonadaceae bacterium strain ING2-E5B isolated from a mesophilic lab-scale biogas reactor. J Biotechnol [Internet]. 2015;193:34–6. Available from: http://dx.doi.org/10.1016/j.jbiotec.2014.11.010

25. Jung S, Regan JM. Comparison of anode bacterial communities and performance in microbial fuel cells with different electron donors. Appl Microbiol Biotechnol. 2007;77(2):393–402.

26. Bond DR. Electrode-Reducing Microorganisms That Harvest Energy from Marine Sediments. Science (80-) [Internet]. 2002;295(5554):483–5. Available from: http://www.sciencemag.org/cgi/doi/10.1126/science.1066771

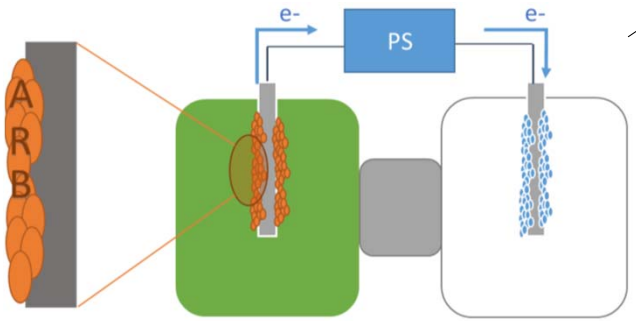

Electro-Selective Fermentation (ESF)

6-d → 2-d SRT

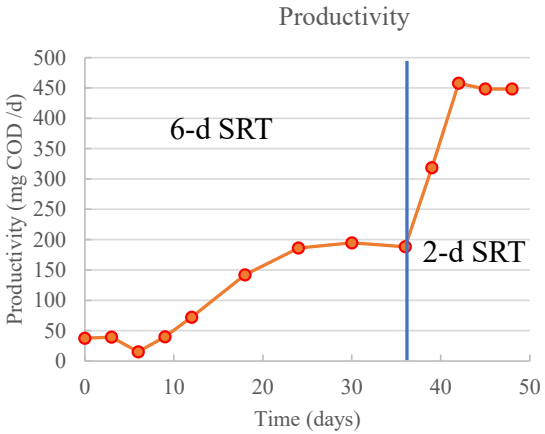

Lipid Extraction ↓

Lipid loss ↓

Total production ↑

MEC-A

2-d → 6-d SRT

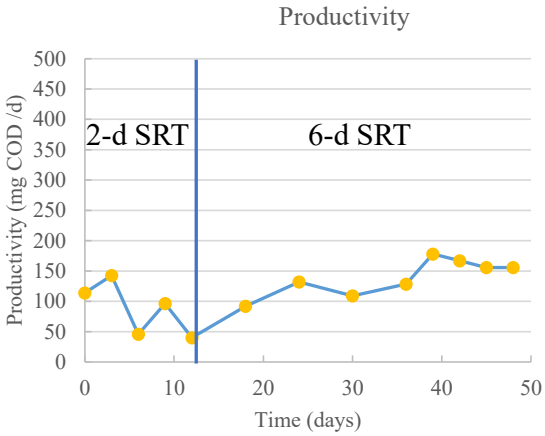

Lipid Extraction ↑

Lipid loss ↑

Total production ↓

MEC-B